

What has quenched the massive spiral galaxies?

Yu Luo¹,¹★ Zongnan Li,² Xi Kang,^{1,3}★ Zhiyuan Li² and Peng Wang^{1,4}

¹Purple Mountain Observatory, No. 10 Yuanhua Road, Nanjing 210033, China

²School of Astronomy and Space Science, Nanjing University, Nanjing 210093, China

³Zhejiang University–Purple Mountain Observatory Joint Research Center for Astronomy, Zhejiang University, Hangzhou 310027, China

⁴Leibniz-Institut für Astrophysik Potsdam (AIP), An der Sternwarte 16, D-14482 Potsdam, Germany

Accepted 2020 May 22. Received 2020 May 22; in original form 2020 March 3

ABSTRACT

Quenched massive spiral galaxies have attracted great attention recently, as more data are available to constrain their environment and cold gas content. However, the quenching mechanism is still uncertain, as it depends on the mass range and baryon budget of the galaxy. In this letter, we report the identification of a rare population of very massive, quenched spiral galaxies with stellar mass $\gtrsim 10^{11} M_{\odot}$ and halo mass $\gtrsim 10^{13} M_{\odot}$ from the Sloan Digital Sky Survey at redshift $z \sim 0.1$. Our CO observations using the IRAM (Institute for Radio Astronomy in the Millimeter Range) 30-m telescope show that these galaxies contain only a small amount of molecular gas. Similar galaxies are also seen in the state-of-the-art semi-analytical models and hydrodynamical simulations. It is found from these theoretical models that these quenched spiral galaxies harbour massive black holes, suggesting that feedback from the central black holes has quenched these spiral galaxies. This quenching mechanism seems to challenge the popular scenario of the co-evolution between massive black holes and massive bulges.

Key words: galaxies: evolution – galaxies: spiral – galaxies: star formation.

1 INTRODUCTION

Galaxies are complex ecosystems composed of dark matter and multiphase baryonic components, where gas accretion, cooling, star formation, and feedback occur on different physical scales (Tumlinson, Peebles & Werk 2017). Overall, galaxies display a clear bimodal distribution in the colour–stellar mass or colour–morphology diagram, in the sense that massive galaxies are mostly red and bulge dominated, while low-mass ones have blue colours with discy morphologies (e.g. Blanton et al. 2003). However, there is a rare population of galaxies that are quenched in their star formation, albeit with discy morphologies. Quenched spiral galaxies have been noticed for a long time (e.g. van den Bergh 1976; Couch et al. 1998) and received more attention in recent years with the advent of large sky surveys (e.g. Masters et al. 2010; Rowlands et al. 2012; Fraser-McKelvie et al. 2018; Hao et al. 2019; Mahajan et al. 2020). However, most existing studies have focused on observational facts rather than the quenching mechanism, in particular in the case of massive, group-central spiral galaxies.

To quench star formation in a massive galaxy, all channels leading to the accumulation of copious molecular gas have to be shut down (Man & Belli 2018). Unlike satellite galaxies whose cold gas can be relatively easily removed by environmental effects, quenching

of central spiral galaxies is more complicated. Quenching does not necessarily mean that cold gas is absent. For example, Zhang et al. (2019) showed that quenched spiral galaxies with stellar mass in the range of $10^{10.6} M_{\odot} < M_{*} < 10^{11} M_{\odot}$ at $0.02 < z < 0.05$ have HI mass around $10^{10} M_{\odot}$, which is systematically higher than that of elliptical galaxies with similar stellar masses. This result suggests that the prevalence of diffuse HI gas is the main reason for preventing continuous star formation. However, it is not without controversy; for instance, Cortese et al. (2020) recently reported that the bulk of passive disc galaxies in the GALEX Arecibo SDSS Survey (xGASS; Catinella et al. 2018) are still HI-poor across the stellar mass range of $10^9 < M_{*}/M_{\odot} < 10^{11}$.

In addition to the uncertain existence of cold gas (either molecular or hydrogen) in quenched central spiral galaxies, the need for quenching depends on the halo mass and the baryon budget in the galaxy. For example, Li et al. (2019) studied a massive isolated spiral galaxy, NGC 5908, which is considered inactive in star formation. By measuring various baryonic components, they concluded that this galaxy is ‘missing baryon’, not completely quiescent, and probably at an early evolutionary stage after a fast growth stage. This kind of baryon-deficient galaxies may be the progenitors of the local massive quenched spiral galaxies. This scenario circumvents extra feedback to suppress gas cooling, but it has to face the missing baryon problem. However, Posti, Fraternali & Marasco (2019) found that most massive central spirals with stellar masses below $10^{11} M_{\odot}$ are living in medium-mass haloes (a few times $10^{12} M_{\odot}$),

* E-mail: luoyu@pmo.ac.cn (YL); kangxi@zju.edu.cn (XK)

where almost all the halo gas has cooled and turned into stars in the disc. These results indicate that the observational uncertainty in the halo mass may affect the explanation.

Overall, from the observational aspects, the formation route of massive quenched spiral galaxies is still unclear. Nevertheless, for galaxies in massive haloes (more than $10^{13} M_{\odot}$), most baryon is in the hot gaseous halo with a quasi-universal fraction (e.g. Wang et al. 2017; Davies et al. 2020). In this mass regime, unless cooling of the hot gas is suppressed, the central galaxy will get replenishment of its cold gas for continuous star formation. A few mechanisms have been proposed to suppress gas cooling, among which active galactic nucleus (AGN) heating is the most common solution (Di Matteo, Springel & Hernquist 2005; Croton et al. 2006; Cattaneo et al. 2009). Powerful AGN feedback requires the existence of a massive black hole. However, according to the bulge–black hole co-evolution scenario, a spiral galaxy without a prominent bulge is unlikely to host a massive black hole. This poses a challenging question: What has quenched these massive central spiral galaxies? Based on the lambda cold dark matter cosmology, the state-of-the-art semi-analytical models (SAMs) and hydrodynamical simulations [e.g. L-Galaxies (Guo et al. 2011; Henriques et al. 2015, hereafter H15); EAGLE simulation (Crain et al. 2015; Schaye et al. 2015); and IllustrisTNG simulation (Nelson et al. 2018; Pillepich et al. 2018; Springel et al. 2018)] have successfully reproduced many observations. It is then interesting to see whether they can predict the existence of quenched massive spiral galaxies.

In this letter, we report our investigation of a rare population of massive quenched central spiral galaxies, which are identified from the Sloan Digital Sky Survey (SDSS). Among them, we have selected four galaxies to probe the amount of molecular gas with the IRAM (Institute for Radio Astronomy in the Millimeter Range) 30-m telescope. By investigating the existence of such galaxies in both the state-of-the-art SAM and hydrodynamical simulations, we propose the most plausible formation scenario.

2 SAMPLE SELECTION

We identify a rare population of quenched massive spiral galaxies from the publicly available galaxy group catalogue (Yang et al. 2012) constructed from the SDSS Data Release 7 (Abazajian et al. 2009). First, we select disc-dominated central galaxies with the criterion of $\text{fracDev}_r < 0.1$, where fracDev_r is the coefficient of the de Vaucouleurs component, which is a good indicator of the bulge-to-total mass ratio. These galaxies are then separated into star-forming and quenched ones via the specific star formation rate $\text{sSFR} = \text{SFR}/M_*$ with a threshold of 10^{-11} yr^{-1} . In this work, the sSFRs of galaxies are from Chang et al. (2015), which combines optical (SDSS) and infrared (Wide-field Infrared Survey Explorer; Wright et al. 2010) photometry. At this point, we have 16 335 central spiral galaxies, most of which are star-forming galaxies (Fig. 1). We then select those in massive haloes $M_{\text{halo}} \geq 10^{13} h^{-1} M_{\odot}$, resulting in 72 discy central galaxies. Among them, there are 27 quenched galaxies with stellar mass around $2 \times 10^{11} M_{\odot}$, which is larger than the quenched galaxies studied in some previous work (e.g. Zhang et al. 2019). For comparison, we also use a mass-dependent sSFR threshold (Trussler et al. 2020) to separate star-forming and quenched galaxies. It is found that the majority of these 27 galaxies are still classified as quenched; only 5 galaxies (marked with crosses in Fig. 1) become star forming, but they still belong to the green valley according to the Trussler et al. (2020) threshold.

These 27 quenched discy galaxies are all found in isolated environment: their distances to the nearest central galaxy are larger

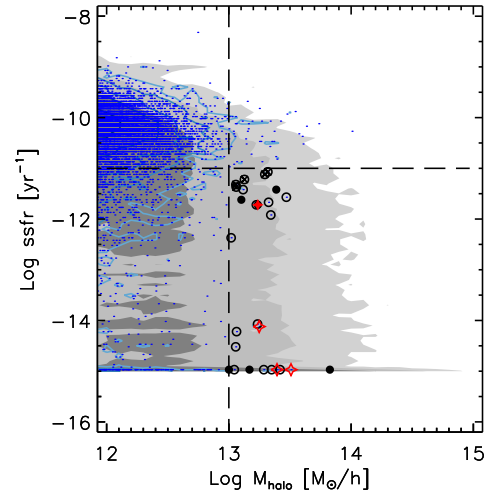


Figure 1. The sSFR–halo mass distribution of central spiral galaxies in the SDSS. The dark and grey shadow shows the sSFR–halo mass distribution of all the central galaxies in our SDSS catalogue. The blue contours show those 16 335 central galaxies with $\text{fracDev}_r < 0.1$. The rest of the symbols (circles and stars) are our 27 quenched massive central spiral samples. Among them, six galaxies showing AGN activity according to the Baldwin, Phillips & Telervich (BPT) diagram are marked by the filled symbols, five galaxies that are above the quenched threshold of Trussler et al. (2020) are marked with open circles plus crosses, and four galaxies observed by the IRAM 30-m telescope are marked by red stars. The horizontal and vertical dashed lines are our criteria to select quenched and massive galaxies.

than 1 Mpc and their group richness is less than 5. It suggests that they are not living at the outskirts of nearby overdense region where environmental quenching may be effective. In other words, these galaxies are quenched either because they lack new cold gas supply or because there is a reservoir of cold gas, but the star formation is suppressed by certain mechanism. Thus, probing other forms of baryonic mass other than stellar mass is the key to understand why these galaxies are quenched.

We have searched for signs of AGN activities from publicly available data bases, in the radio [FIRST (Becker, White & Helfand 1995), NVSS (Condon et al. 1998), and LOFAR (van Haarlem et al. 2013)] and X-ray (Chandra, *XMM-Newton*) bands, but found no counterpart for any of the sample galaxies. This is consistent with our finding from the BPT diagram that only 6 of the 27 galaxies show weak AGN activities (marked by the filled symbols in Fig. 1).

We have also looked for detections of H I or molecular gas using the ALFALFA (Haynes et al. 2018) and xCOLD GASS (Saintonge et al. 2017) surveys. All but one galaxy in our sample have redshifts larger than 0.1, with one at $z \sim 0.08$. Unfortunately, galaxies in the two surveys have redshifts lower than 0.06, far less than the redshift range of our samples. However, a recent study (Zhang et al. 2019) shows that quenched spiral galaxies with stellar mass $10^{10.6} M_{\odot} < M_* < 10^{11} M_{\odot}$ at $0.02 < z < 0.05$ have H I mass around $10^{10} M_{\odot}$, systematically higher than that of elliptical galaxies with similar mass. The stellar mass–halo mass relation from the abundance matching (Moster, Naab & White 2013) suggests that the quenched galaxies of Zhang et al. (2019) are living in haloes with $M_{\text{halo}} < 3 \times 10^{12} M_{\odot}$, well below our selection of halo mass above $10^{13} h^{-1} M_{\odot}$.

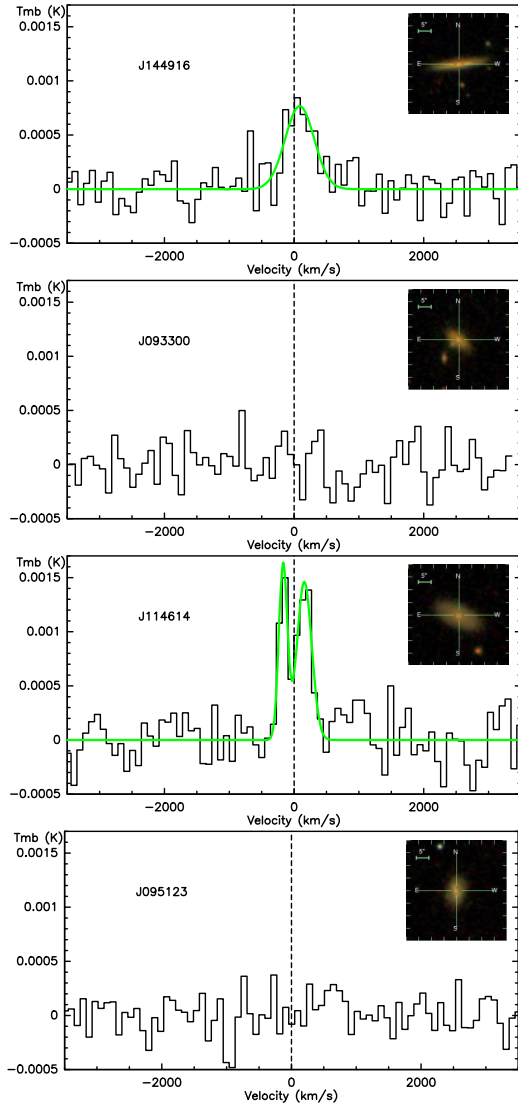


Figure 2. The CO(1–0) spectra of four selected massive central spirals, the SDSS image of which is displayed in the inset. For the two galaxies with significant CO(1–0) emission, one or two Gaussians are applied to fit the spectra and the results are shown by the green curve. The vertical dashed line indicates the corresponding redshift of each galaxy.

3 CO OBSERVATION

To put a rough limit on the amount of molecular gas in these quenched galaxies, we select 4 galaxies from our sample of 27 galaxies to carry out CO observations using the IRAM 30-m telescope. The four targets are chosen for an optimal combination of distance, sSFR, and morphology. The SDSS images of the four galaxies are shown in the inset of each panel in Fig. 2, and their basic properties are given in Table 1. The first galaxy, SDSS J144916, is an edge-on galaxy showing a clear discy morphology. The other three galaxies have extended discs and visible small bulges.

Detailed information of the CO observations and the fitting results of the derived spectra are given in Table 1. The individual CO spectra and the fitted Gaussian models (for detection only) are shown in Fig. 2. Only two galaxies, SDSS J144916 and SDSS J114614, show a significant CO(1–0) line at a confidence level greater than 3σ . The line intensity is converted from main beam temperature T_{mb}

(K) to flux density S (Jy) using $S/T_{\text{mb}} \sim 5 \text{ Jy K}^{-1}$ at 100 GHz.¹ The CO line luminosity L_{CO} is then calculated following the standard equation from Solomon et al. (1997):

$$L_{\text{CO}} = 3.25 \times 10^7 S_{\text{CO}} \Delta V v_{\text{obs}}^{-2} D_L^2 (1+z)^{-3}, \quad (1)$$

where L_{CO} is in units of $\text{K km s}^{-1} \text{ pc}^2$, the CO flux $S_{\text{CO}} \Delta V$ obtained with Gaussian fitting is in units of Jy km s^{-1} , the observing frequency ν_{obs} is in GHz, and the luminosity distance D_L is in Mpc. We adopt the fiducial CO-to- H_2 conversion factor $\alpha_{\text{CO}(1-0)} = 4.35 \text{ M}_{\odot} \text{ pc}^{-2} (\text{K km s}^{-1})^{-1}$, equivalent to $X_{\text{CO}} = 2 \times 10^{20} \text{ cm}^{-2} (\text{K km s}^{-1})^{-1}$ (e.g. Bolatto, Wolfire & Leroy 2013) to convert CO luminosity to molecular gas mass. However, we note that this conversion factor is of large uncertainty, especially for the rare sample of massive quenched central spirals. For the two sources without a significant CO detection, we estimate the 3σ upper limit by assuming a line width FWHM of 500 km s^{-1} , similar to the observed values.

All the four galaxies have amount of molecular gas less than $1.2 \times 10^{10} \text{ M}_{\odot}$. The molecular gas fraction (M_{H_2}/M_*) is $\lesssim 4$ percent in three galaxies and ~ 8 percent in the remaining galaxy (SDSS J114614). For the two galaxies with CO detection, the circular velocity can be approximated by the 20 percent peak line width of the spectra and certain inclination angle, which are 274.7 and 283.2 km s^{-1} for SDSS J144916 and SDSS J114614, respectively. Assuming a typical NFW profile (Navarro, Frenk & White 1997) and the halo mass–concentration relation (Prada et al. 2012), we can estimate halo mass by fitting the circular velocity at the radius within which the CO is detected. We obtain similar halo mass of $10^{13.1} \text{ M}_{\odot}$ for both the galaxies. Note that here this mass is the lower limit as we assumed that the size of molecular gas extends to the stellar disc. Adopting an equal upper limit of $10^{10} \text{ M}_{\odot}$ for both H I and molecular gas for our galaxies, the gas fraction is at most 10 percent. Thus, we do discover a rare population of quenched spiral galaxies with stellar mass around $2 \times 10^{11} \text{ M}_{\odot}$ and a small fraction of cold gas, living in haloes more massive than $10^{13} h^{-1} \text{ M}_{\odot}$.

4 THEORETICAL MODELS FOR GALAXY FORMATION

Both the SAMs and hydrodynamic simulations are powerful tools to study galaxy formation and evolution in a cosmological context. We examine the state-of-the-art SAMs and hydrodynamic simulations to see whether they are able to predict the existence of galaxies analogous to our sample galaxies, and if any, to shed light on the cause of quenching in these massive spiral galaxies.

4.1 Semi-analytical model

SAMs are usually based on merger trees from N -body simulations and incorporate phenomenological descriptions of various physical processes related to galaxy formation, such as cosmic reionization, hot gas cooling and cold gas infall, star formation and metal production, supernova feedback, gas stripping and tidal disruption of satellites, galaxy mergers, bulge formation, black hole growth, AGN feedback, etc. They can reproduce lots of observational facts such as the mass/luminosity function, the galaxy colour–mass diagram, and so on. L-Galaxies is one of the most successful semi-analytical galaxy formation models, which has been continuously

¹<http://www.iram.es/IRAMES/mainWiki/Iram30mEfficiencies>

Table 1. Basic information and observation log of our target galaxies.

Name	J144916.71+150700.1	J093300.93+594420.4	J114614.24+111501.7	J095123.60+265643.9
RA (J2000)	222.320	143.254	176.559	147.848
Dec. (J2000)	15.117	59.739	11.251	26.946
z	0.111	0.151	0.114	0.131
$\log M_{\text{halo}} (M_{\odot})^a$	13.40	13.55	13.66	13.29
$\log M_{*} (M_{\odot})^b$	11.20	11.29	11.12	11.02
$\log \text{sSFR} (\text{yr}^{-1})^c$	-14.12	-14.97	-14.97	-11.72
Frequency (GHz)	103.75	100.15	103.48	101.92
$T_{\text{int}} (\text{h})^d$	4.5	5	3	4.4
rms ^e (mK)	0.15	0.17	0.22	0.15
Velocity ^f (km s ⁻¹)	82.47 ± 34.21	–	-169.40 ± 12.31 157.77 ± 17.30	–
FWHM ^g (km s ⁻¹)	547.74 ± 100.90	–	155.36 ± 36.09 267.31 ± 43.26	–
$T_{\text{mb,peak}}^h$ (mK)	0.93 ± 0.15	–	1.95 ± 0.22 1.76 ± 0.22	–
I_{CO}^i (K km s ⁻¹)	0.54 ± 0.07	<0.31 ^j	0.33 ± 0.06 0.51 ± 0.07	<0.28 ^j
$\log L_{\text{CO}} (L_{\odot})^k$	9.20 ± 0.06	< 9.24	9.41 ± 0.05	< 9.06
$\log M_{\text{H}_2,\text{o}} (M_{\odot})^l$	9.84 ± 0.06	< 9.88	10.05 ± 0.05	< 9.70
$\log M_{\text{gas,p}} (M_{\odot})^m$	9.98	10.02	9.95	9.91

^aHalo mass from Yang et al. (2012) group catalogue.

^bStellar mass from Chang et al. (2015) catalogue.

^csSFRs from Chang et al. (2015) catalogue.

^dIntegration time.

^eThe baseline rms in 90 km s⁻¹ channel.

^fCentral velocity.

^gFull width at half-maximum.

^hPeak main beam temperature.

ⁱIntegrated intensity.

^j3 σ upper limit by assuming a line width of 500 km s⁻¹.

^kCO luminosity.

^lObserved molecular gas mass.

^mPredicted cold gas mass from H15.

developed by the Munich group in the last two decades. H15 presented the latest L-Galaxies model, in which they have used the Markov chain Monte Carlo method to search the parameter space, successfully fitting the evolution of stellar mass function and the overall fraction of red galaxies from $z = 3$ to 0.

Here, we use the public catalogue² of H15 implemented on the Millennium Simulation (Springel et al. 2005). Following the sample selection from the SDSS, we select central galaxies at $z = 0.1$ with $M_{\text{halo}} > 10^{13} h^{-1} M_{\odot}$ and $B/T = M_{\text{bulge}}/M_{*} < 0.1$ as our criteria for massive spirals. We also use $\log \text{sSFR} = -11 \text{ yr}^{-1}$ to divide these massive central spirals into quenched and star-forming populations. Finally, we obtain 7024 quenched massive central spirals and 372 star-forming ones. There are more quenched galaxies in H15 than in the SDSS catalogue, presumably due to the strong AGN feedback in the H15 model. After checking the different baryonic components of these galaxies in the SAM, we find that the quenched sample has a higher hot gas fraction and a lower cold gas fraction than the star-forming ones. This clearly shows that quenching is directly due to the lack of gas cooling in these massive galaxies. Why, then, the hot gas did not cool? If there were no AGN feedback, both the quenched and star-forming samples would have a similar cooling rate (roughly higher than $200 M_{\odot} \text{ yr}^{-1}$). The SAM suggests that AGN heating is the primary mechanism responsible for quenching the gas cooling and subsequent star formation.

4.2 Hydrodynamic simulation

The IllustrisTNG project is a successful suite of large, cosmological magnetohydrodynamical simulations of galaxy formation that can reproduce many observational results, such as the stellar content distribution (Pillepich et al. 2018), colour distribution (Nelson et al. 2018), and matter and galaxy clustering (Springel et al. 2018). The series of simulation includes three box sizes: 50, 100, and 300 Mpc³ with three different resolutions, respectively. In this work, we use the largest box (TNG300-1), which is suitable for the study of massive galaxies.

We select central galaxies with $M_{*} > 10^{11} M_{\odot}$ from TNG300-1 and decompose their stellar mass distribution into disc and bulge components. Finally, we obtain only eight massive central galaxies with $B/T < 0.2$, all of which are quenched galaxies. To understand why these galaxies are quenched in the model, we show in Fig. 3 the relation between black hole mass and bulge stellar mass from the SAM and IllustrisTNG, respectively. It can be seen that the predicted black hole mass of the eight quenched galaxies is above the empirical black hole mass–bulge mass relation (e.g. Kormendy & Ho 2013; McConnell & Ma 2013), indicating that feedback from the central massive black holes has quenched their star formation.

5 CONCLUSION AND DISCUSSION

From the theoretical point of view, galaxies may still be quenched if they have plenty of cold gas but do not form star efficiently.

²<http://gavo.mpa-garching.mpg.de/Millennium>

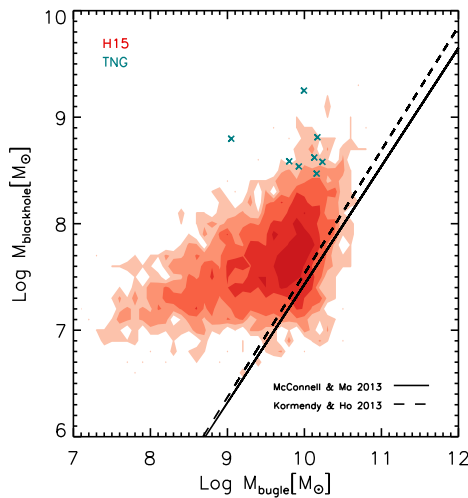


Figure 3. Black hole mass–bulge mass relation for massive spiral galaxies from the H15 SAM and TNG simulation. The red contours and dark green crosses represent the H15 sample (with $M_{\text{halo}} > 10^{13} h^{-1} M_{\odot}$ and $M_{*} > 10^{11} M_{\odot}$) and TNG sample (only with $M_{*} > 10^{11} M_{\odot}$), respectively. The solid line and dashed line are from the classical bulge–black hole mass relation of McConnell & Ma (2013) and Kormendy & Ho (2013).

(i) Dynamical processes related to a bar or bulge can stabilize the gaseous disc from fragmentation. This is ruled out for our observed sample since it requires the galaxies to possess significant bulges. (ii) There is a large diffuse H I gas that cannot form stars directly in these quenched galaxies, as claimed by some recent work (Zhang et al. 2019). Nevertheless, this is refuted by Cortese et al. (2020) that the bulk of the passive disc galaxies in xGASS is still H I-poor across the stellar mass range $10^9 < M_{*}/M_{\odot} < 10^{11}$. (iii) No quenching mechanism is needed if these massive central spirals are living in low-mass haloes (a few times $10^{12} M_{\odot}$), where almost all gas has cooled and turned into stars in the disc, as recently found by Posti et al. (2019). Both the latter cases are possible as galaxies with masses lower than $10^{11} M_{\odot}$ are living in haloes with masses lower than $3 \times 10^{12} M_{\odot}$, where the rapid cold accretion along cosmic filaments is expected (Dekel et al. 2009). This cold gas can be kept in the form of H I gas around the central galaxy or transferred into stars once molecular gas formation becomes efficient. All these indicate that the halo mass is the key to infer the formation of these galaxies. For the massive ones ($> 10^{13} M_{\odot}$), extra strong feedback is necessary.

The galaxies in our sample are more massive ($> 10^{11} M_{\odot}$) and living in haloes massive than $10^{13} h^{-1} M_{\odot}$, where the popular mass or halo quenching term applies. Whatever the mechanism behind the mass quenching, an energy source is needed to balance the cooling of the hot gas (Man & Belli 2018). Our results from both the SAM and IllustrisTNG simulation suggest that the cooling from the hot gaseous halo in these quenched spiral galaxies is suppressed by massive black holes. Other than AGN heating, shock heating from infalling satellites may heat up the gas (Khochfar & Ostriker 2008). In our sample, these galaxies are mostly isolated disc galaxies; thus, mergers should not be important. After excluding these possibilities, we conclude that AGN heating, either still ongoing or being halted shortly before the current epoch, is the most plausible mechanism to suppress gas cooling in these galaxies. This conclusion calls for further careful search of massive black holes in our sample galaxies. The existence of such massive black holes will challenge current scenario of massive black hole formation in bulgeless galaxies,

whereas their non-existence will put more tight constraints on the halo mass and other baryonic components.

ACKNOWLEDGEMENTS

We thank the anonymous referee for useful comments. The Millennium Simulation data bases used in this paper and the web application providing online access to them were constructed as part of the activities of the German Astrophysical Virtual Observatory (GAVO). Based on observations carried out under project number 194-18 with the IRAM 30-m telescope. IRAM is supported by INSU/CNRS (France), MPG (Germany), and IGN (Spain). YL and XK thank partial support for this work by the 973 program (No. 2015CB857003) and the National Natural Science Foundation of China (Nos 11825303, 118611311006, 11333008, and 11703091). ZNL and ZYL acknowledge support from the National Key Research and Development Program of China (2017YFA0402703).

REFERENCES

- Abazajian K. N. et al., 2009, *ApJS*, 182, 543
 Becker R. H., White R. L., Helfand D. J., 1995, *ApJ*, 450, 559
 Blanton M. R. et al., 2003, *ApJ*, 594, 186
 Bolatto A. D., Wolfire M., Leroy A. K., 2013, *ARA&A*, 51, 207
 Catinella B. et al., 2018, *MNRAS*, 476, 875
 Cattaneo A. et al., 2009, *Nature*, 460, 213
 Chang Y.-Y., van der Wel A., da Cunha E., Rix H.-W., 2015, *ApJS*, 219, 8
 Condon J. J., Cotton W. D., Greisen E. W., Yin Q. F., Perley R. A., Taylor G. B., Broderick J. J., 1998, *AJ*, 115, 1693
 Cortese L., Catinella B., Cook R. H. W., Janowiecki S., 2020, *MNRAS*, 494, 42C
 Couch W. J., Barger A. J., Smail I., Ellis R. S., Sharples R. M., 1998, *ApJ*, 497, 188
 Crain R. A. et al., 2015, *MNRAS*, 450, 1937
 Croton D. J. et al., 2006, *MNRAS*, 365, 11
 Davies J. J., Crain R. A., Oppenheimer B. D., Schaye J., 2020, *MNRAS*, 491, 4462
 Dekel A. et al., 2009, *Nature*, 457, 451
 Di Matteo T., Springel V., Hernquist L., 2005, *Nature*, 433, 604
 Fraser-McKelvie A., Brown M. J. I., Pimbblet K., Dolley T., Bonne N. J., 2018, *MNRAS*, 474, 1909
 Guo Q. et al., 2011, *MNRAS*, 413, 101
 Hao C.-N. et al., 2019, *ApJ*, 883, L36
 Haynes M. P. et al., 2018, *ApJ*, 861, 49
 Henriques B. M. B. et al., 2015, *MNRAS*, 451, 2663, (H 15)
 Khochfar S., Ostriker J. P., 2008, *ApJ*, 680, 54
 Kormendy J., Ho L. C., 2013, *ARA&A*, 51, 511
 Li J.-T., Zhou P., Jiang X., Bregman J. N., Gao Y., 2019, *ApJ*, 877, 3
 McConnell N. J., Ma C.-P., 2013, *ApJ*, 764, 184
 Mahajan S. et al., 2020, *MNRAS*, 491, 398
 Man A., Belli S., 2018, *Nat. Astron.*, 2, 695
 Masters K. L. et al., 2010, *MNRAS*, 405, 783
 Moster B. P., Naab T., White S. D. M., 2013, *MNRAS*, 428, 3121
 Navarro J. F., Frenk C. S., White S. D. M., 1997, *ApJ*, 490, 493
 Nelson D. et al., 2018, *MNRAS*, 475, 624
 Pillepich A. et al., 2018, *MNRAS*, 475, 648
 Posti L., Fraternali F., Marasco A., 2019, *A&A*, 626, A56
 Prada F., Klypin A. A., Cuesta A. J., Betancort-Rijo J. E., Primack J., 2012, *MNRAS*, 423, 3018
 Rowlands K. et al., 2012, *MNRAS*, 419, 2545
 Saintonge A. et al., 2017, *ApJS*, 233, 22
 Schaye J. et al., 2015, *MNRAS*, 446, 521
 Solomon P. M., Downes D., Radford S. J. E., Barrett J. W., 1997, *ApJ*, 478, 144
 Springel V., et al., 2005, *Nature*, 435, 629
 Springel V. et al., 2018, *MNRAS*, 475, 676

Trussler J., Maiolino R., Maraston C., Peng Y., Thomas D., Goddard D., Lian J., 2020, *MNRAS*, 491, 5406
Tumlinson J., Peebles M. S., Werk J. K., 2017, *ARA&A*, 55, 389
van den Bergh S., 1976, *ApJ*, 206, 883
van Haarlem M. P. et al., 2013, *A&A*, 556, A2
Wang L., Dutton A. A., Stinson G. S., Macciò A. V., Gutcke T., Kang X., 2017, *MNRAS*, 466, 4858
Wright E. L. et al., 2010, *AJ*, 140, 1868

Yang X., Mo H. J., van den Bosch F. C., Zhang Y., Han J., 2012, *ApJ*, 752, 41
Zhang C. et al., 2019, *ApJ*, 884, L52

This paper has been typeset from a $\mathrm{T}_{\mathrm{E}}\mathrm{X}/\mathrm{L}^{\mathrm{A}}\mathrm{T}_{\mathrm{E}}\mathrm{X}$ file prepared by the author.